  DOI 10.1515/htmp-2011-0150

High-temperature Oxidation Resistance of Al_2O_3-Au Laminated Composite Coating Prepared on TiAl-based Alloy

Xiaoxu Ma,[1] **Yedong He,**[1,*] **Deren Wang,**[1] **Junpin Lin**[1] **and Wei Gao**[2]

[1] State Key Laboratory for Advanced Metals and Materials, University of Science and Technology Beijing, Beijing, China

[2] Engineering School, the University of Auckland, Auckland, New Zealand

Abstract. Novel composite coatings consist of Al_2O_3 micro-layers alternating with Au nano-layers have been prepared on TiAl-based alloy by magnetron sputtering. The results of high-temperature cyclic oxidation test at 900 °C for 200 h revealed that the multi-sealed α-Al_2O_3 and Au layers effectively suppress the inward diffusion of oxygen to a low level. The formed oxide scales and composite coatings are compact and free of cracks. The thermal stress is decreased owing to the increase of thermal-expansion coefficient. And the surface scratch test exhibited that the brittle/ductile laminated structure can remarkably enhance the strength and toughness in combination with improved damage resistance of the Al_2O_3-Au laminated composite coatings. Consequently, the oxidation and spallation resistance of TiAl-based alloy have been improved significantly.

Keywords. Magnetron sputtering, titanium aluminides, laminated coating, cyclic oxidation, high-temperature, mechanical properties testing.

PACS®(2010). 68.65.Ac.

1 Introduction

TiAl alloys are highly promising for high-temperature structural applications in the area of astronautics and aeronautics because of their attractive properties such as low density, high melting temperature and high-temperature strength. However, the oxidation resistance of TiAl alloys is very poor at high temperatures (≥800 °C) due to the fact that they can't form long-lasting protective alumina scales [1–4]. Previous researches [5–8] pointed out that the high-temperature oxidation resistance of TiAl alloys could be effectively improved by addition of the minor alloying elements which can favor the formation of alumina scale. Besides, various coatings including alloy coatings [1, 9, 10], thermal barrier coatings [12, 13] and ceramic coatings [14–16] of surface protection for TiAl alloys have been widely proposed and investigated. However, spallation of such coatings after high-temperature cyclic oxidation [11, 17] has become a critical problem hindered their application because cracking and spalling of the formed oxide scales and ceramic coatings cannot be avoided completely [18, 19]. Therefore, new coating systems providing great oxidation and excellent spallation resistance for TiAl alloys have to be developed.

It is widely known that one effective way to improve the durability, strength and fracture toughness of ceramics is to form a composite material [20]. So, it is reasonable to propose that the coatings with a composite structure should possess improved mechanical properties than that with a single phase coating. Such coatings can be fabricated by reinforcing the brittle ceramic matrix with a high-modulus, high-strength or high-ductility second constituent in the form of multi-layers, fibres, platelets or particulates [21]. Recent researches have shown that the ceramic coatings with brittle/brittle laminated composite structures can effectively resist scale spallation and oxidation at high temperatures. He et al. [22–24] have developed different ways to prepare the ZrO_2-Al_2O_3 micro-laminated structural coatings which exhibit great oxidation and spallation resistance at high temperatures because of the oxygen diffusion suppression of multi-sealed Al_2O_3 layers and the crack resistance of the brittle/brittle laminated structure [25]. While, for the composite coatings with alternating high-strength ceramic layers and high-ductility metal layers, it seems that only few reports have been dedicated to the hightemperature oxidation and spallation resistance of such brittle/ductile laminated coatings as protective coatings so far.

Based on the above research, a novel Al_2O_3 (A)-Au (G) laminated composite coating is proposed as a high-temperature protective coating for TiAl-based alloy in this study. We expect that the brittle Al_2O_3 layers can maintain the composite coating high strength and the ductile Au layers probably can shield the crack tip by the plastic deformation of ductile ligaments. The Al_2O_3 [26, 27] and Au both have very low oxygen diffusion rates, which may give su-

* **Corresponding author:** Yedong He, State Key Laboratory for Advanced Metals and Materials, University of Science and Technology Beijing, Beijing, China;
E-mail: htgroup@mater.ustb.edu.cn.

Received: August 31, 2011. Accepted: December 20, 2011.

perior oxidation resistance to the laminated coating. Moreover, the Al_2O_3 and Au laminated layers are deposited atom by atom in magnetron sputtering (MS) system. Therefore, the microstructure of deposited layers can be modified by controlling the deposition parameters of MS in this work. It is reasonable to expect that the A-G laminated composite coating can provide good oxidation and spallation resistance.

2 Experimental

The TiAl-based alloy prepared by vacuum melting method was used as the substrate material with a composition (mass %) of 8% Nb, 45% Al, 0.1% Y, 0.2% W, balance Ti. The TiAl-based alloy was processed into cuboids ($15 \times 10 \times 3$ mm^3). All surfaces of the prepared substrates were mechanically polished using SiC paper up to a grit of 2000 and then ultra-precision polished (Ra $= 0.03$ μm), followed by ultrasonic cleaning with ionized water and ethanol, respectively.

The Al_2O_3-Au (A-G) laminated composite coatings were fabricated in an opposite-targets MS system (Model TUS-800MP) as shown in Figure 1. The chamber was evacuated to a base pressure of 3.0×10^{-3} Pa and the working gas argon was flown into the chamber till the working pressure reached 0.5 Pa. The substrates were fixed on a rotating specimen holder (the rotation speed is ∼20 rpm) to ensure that all the surfaces of the substrates can be deposited. The A-G laminated composite coatings were fabricated as follows. First, the bottom Al_2O_3 layer was deposited on the substrates by radio frequency (RF) MS using a 2 in. diameter α-Al_2O_3 ceramic target (purity >99.99 %) at 120 °C (substrate temperature). The chosen of RF power and deposition period were 150 W and 5 h respectively. The Al_2O_3 layer rather than the Au layer was firstly deposited as the bottom layer of the laminated coatings mainly because it can be considered as an intermediate film preventing mutual diffusion between the substrate and the laminated coating at high temperatures. Then, an Au layer was deposited on the bottom Al_2O_3 layer by direct current (DC) MS using a 2 in. diameter Au metallic target (purity >99.99%) for 2 min at 200 mA, 0.8 kV. By this means, Al_2O_3 and Au layers were prepared alternately on the substrate. Finally, A-G laminated composite coatings with three layers (A/G/A) and five layers (A/G/A/G/A) were prepared on TiAl-based alloy in this study. Besides, a single Al_2O_3 coating was also deposited on the TiAl-based alloy by RF MS at 150 W for 20 h. To release the inner stress generated during the preparation procedure, all the prepared coatings were annealed at 300 °C in Ar for 2 h.

Cyclic oxidation tests of samples (Table 1) were performed in a horizontal furnace at 900 °C in laboratory air for 200 h at atmospheric pressure. After a certain oxidation period of 10 h, the samples placed in the constant

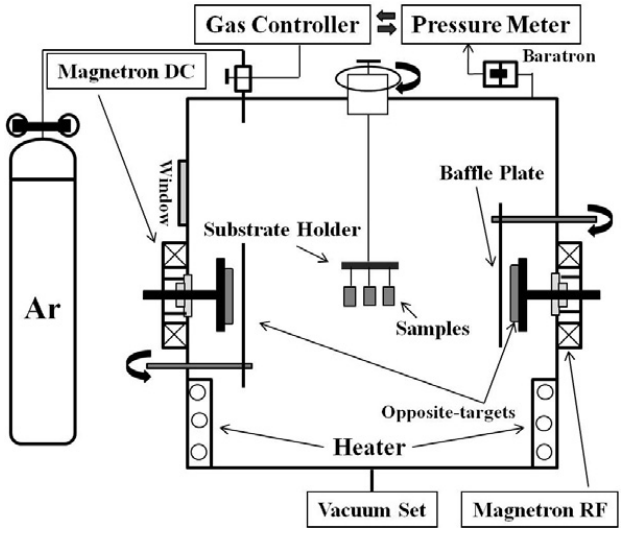

Figure 1. Schematic diagram of the opposite-targets MS system.

mass quartz crucibles were taken out and cooled to room temperature. Then, the mass gain (specimen + crucible) and spallation mass (crucible) of samples were weighed using an electronic balance with an accuracy of 10^{-5} g. After the measurement, samples were put back to the heating zone. This oxidation test providing 20 times thermal cycles can accurately evaluate thermal shock resistance of the A-G laminated composite coatings.

The morphology and composition of the deposited coatings and the formed oxide scales were characterized by high-resolution field emission scanning electron microscopy (FE-SEM) with an energy-dispersive spectroscopy (EDS) system. Phases of the oxide scales were identified using X-ray diffraction (XRD) (Rigaku-D/max-RB, X-ray diffractometer with Cu Kα radiation, $\lambda = 0.1546$ nm, 12 kW, 40 kV, 150 mA step width 0.02°–10° min^{-1}).

A multi-functional material surface testing machine (model MFT-4000) was used to study the adhesion of the formed oxide scales on samples after the oxidation test at room temperature.

3 Results

3.1 Surface and Cross-sectional Morphologies of Coatings

Figure 2 shows the surface and cross-sectional morphologies of the deposited single Al_2O_3 coating (Figure 2 (a) and 2 (b)), three layers (Figure 2 (c) and 2 (d)) and five layers (Figure 2 (e) and 2 (f)) A-G laminated composite coatings, respectively. Furthermore, it is seen from the surface images that the surfaces of all the deposited coatings are compact and no cracks are observed. The cross-sectional images

Sample No.	Substrate	Surface coating
1	TiAl-based alloy	None
2	TiAl-based alloy	Single Al_2O_3 coating
3	TiAl-based alloy	Three layers A-G laminated composite coating
4	TiAl-based alloy	Five layers A-G laminated composite coating

Table 1. The composition of the samples.

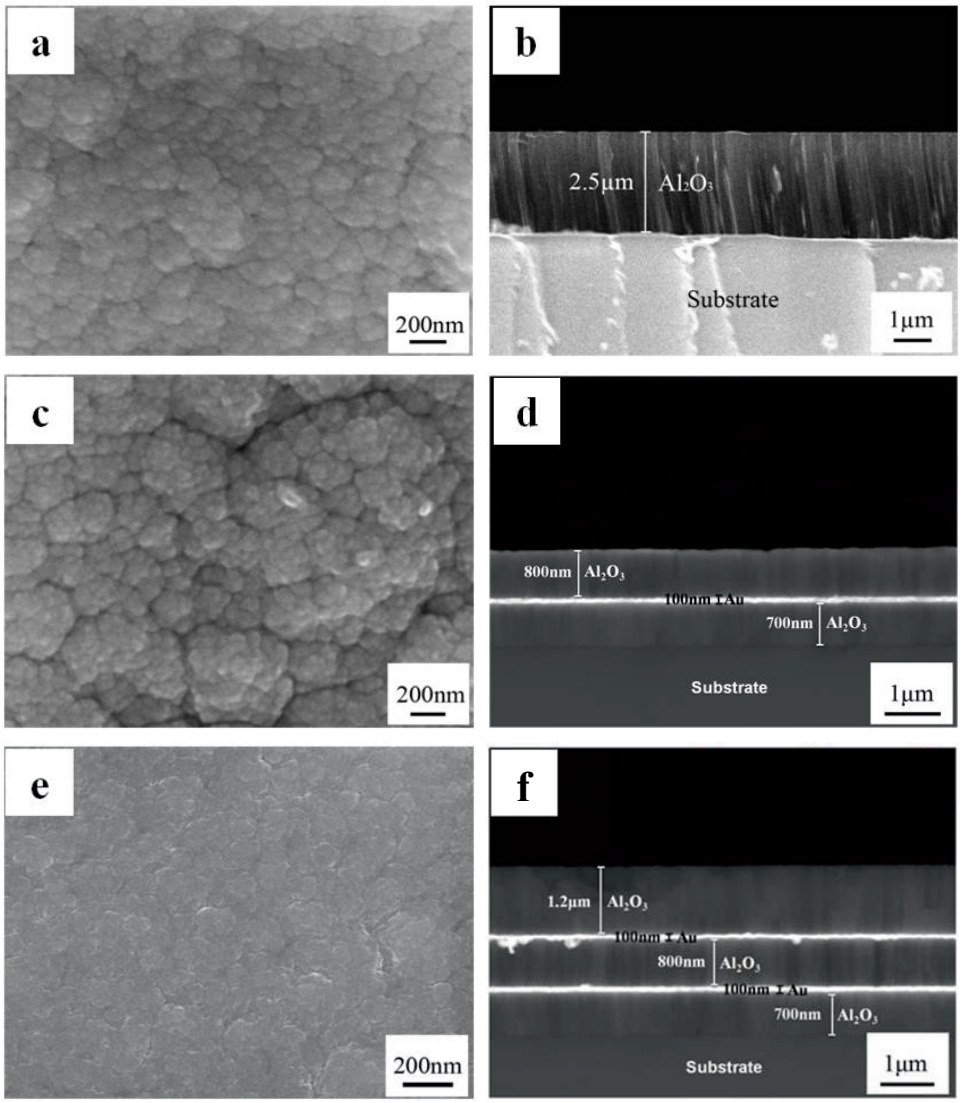

Figure 2. SEM images of coatings prepared by MS: single Al_2O_3 coating (a) surface, (b) cross-section; three layers A-G laminated composite coating (c) surface, (d) cross-section and five layers A-G laminated composite coating (e) surface, (f) cross-section.

of coatings show that the single Al_2O_3 coating and the five layers A-G laminated coating both have a thickness of ~2.5 μm while the thickness of three layers A-G laminated coating is ~1.5 μm. All the coatings show a good adhesion with the substrate. Also, it can be viewed that the defects are effectively avoided and the Al_2O_3 and Au layers are dense, continuous and bond with each other tightly, indicating the complete isolation of substrates.

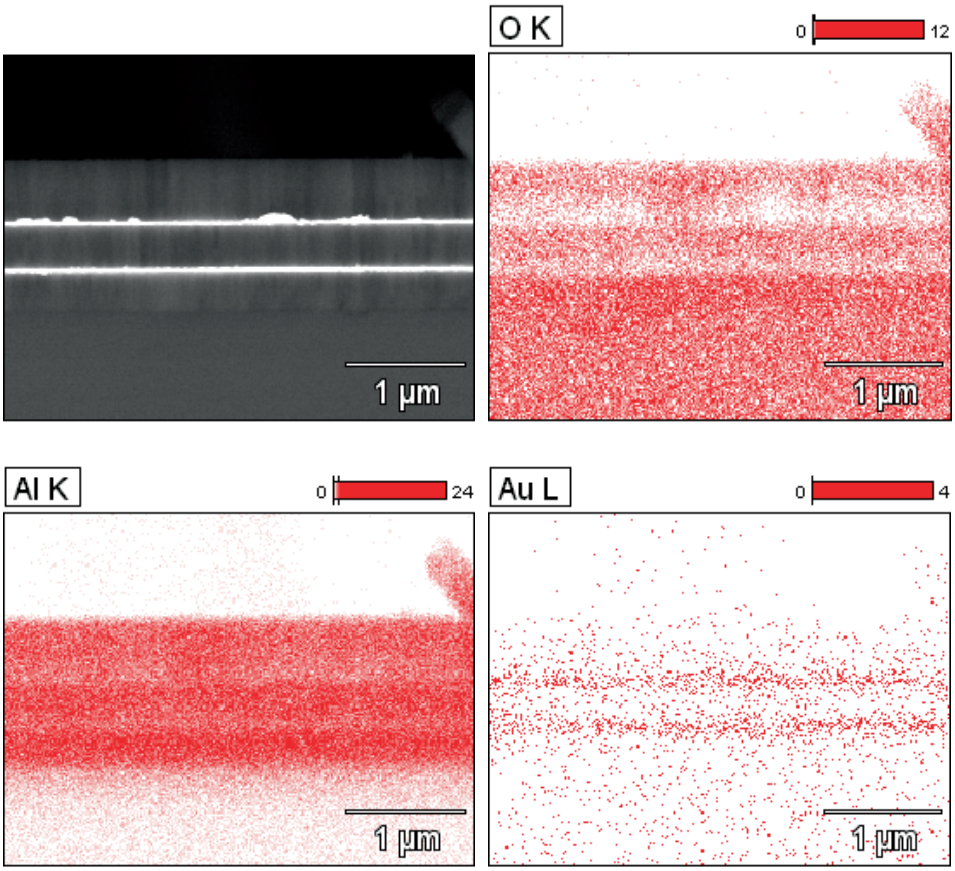

Figure 3. Element area distributions of five layers A-G laminated composite coating prepared by MS.

The XRD result (not given) of the coatings before high-temperature oxidation test shows that the deposited Al_2O_3 is an amorphous phase. In addition, the element area distribution of the 5-layer laminated coating is shown in Figure 3.

3.2 Cyclic High-temperature Oxidation Test of Coatings on TiAl-based Alloy Substrate

Figure 4 shows the oxidation kinetics results of the samples uncoated and coated with a single Al_2O_3 coating, three layers and five layers A-G laminated composite coatings after cyclic oxidation test. It can be seen that all the prepared coatings can improve the oxidation and spallation resistance of the TiAl-based alloy. While compared with the single Al_2O_3 coating, the three layers and five layers A-G laminated composite coatings show much better high-temperature spallation and oxidation resistance. The weight gain and spallation mass of the sample coated with five layers A-G laminated composite coating are both the least, which are 1.3 mg/cm^2 and 1.0 mg/cm^2, respectively. Consequently, five layers A-G laminated composite coating exhibits the best high temperature performance. So, it could be concluded that the more layers the laminated coating has, the better spallation and oxidation resistance it provides.

3.3 Characterization of Samples after Cyclic High-temperature Oxidation Test

Surface morphologies and cross-sectional images of samples after cyclic oxidation are shown in Figure 5. The uncoated sample exhibits a very porous surface (Figure 5 (a)) and an Nb-rich layer instead of an oxide scale is observed in Figure 5 (b). The entirely spallation of the oxide scale can be attributed to the strong interface stress caused by the huge difference of the thermal-expansion coefficient (CTE) between oxide scale and substrate. According to the experimental results, the deposited single Al_2O_3 coating can only slightly improve the high-temperature oxidation and spallation resistance of TiAl-based alloy because the transformed α-Al_2O_3 layer from the deposited amorphous Al_2O_3 layer was destroyed (Figure 5 (c) and 5 (d)) and failed preventing the diffusion of oxygen due to the poor Al_2O_3-TiAl chemical and physical capability.

In addition, the cyclic oxidation test results of samples coated with three and five layers A-G laminated coatings are compared and discussed. Surface morphologies (Figure 5 (e) and 5 (g)) show that the sample coated with five layers A-G laminated coating displays much denser and smoother surface morphology with less TiO_2 and much

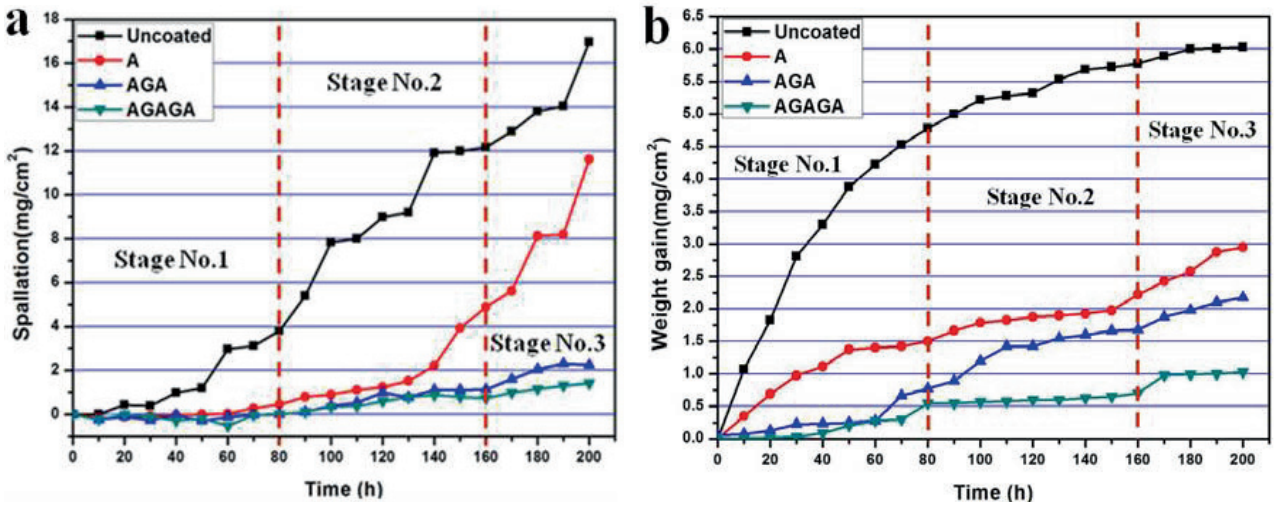

Figure 4. Oxidation kinetics of uncoated TiAl-based alloy and coated with a single Al_2O_3 coating, three layers and five layers A-G laminated composite coatings TiAl-based alloy samples at 900 °C in air for 200 h: (a) Spallation mass vs. time; (b) Weight gain vs. time.

smaller TiO_2 grain size. This reveals that the five layers A-G laminated coating more effectively suppresses the inward oxygen diffusion and inhibits the selective oxidation of Ti. Comparing with Al, the diffusion of Ti in coating is faster and it is easier to be oxidized. So, when Ti reaches the surface of the coating, it will be oxidized to TiO_2. Cross-sectional images (Figure 5 (f) and 5 (h)) show that a continuous and dense α-Al_2O_3 layer has been formed from the deposited amorphous Al_2O_3 layers in the oxide scales of the samples coated with three and five layers A-G laminated coatings. Besides, it is viewed that the sample coated with three layers A-G laminated coating is oxidized severer as its oxide scale and external TiO_2 layer are both thicker. Please indicate the external TiO_2 layer in Figure 5 (f). How does the external TiO_2 layer form?

An interesting observation in Figure 5 (f) and 5 (h) is that the Au nano-layers are replaced by Au particles and platelets which distributed in the α-Al_2O_3 layer after the oxidation test. This might be explained that the continuous growth of the coating inner stresses generated by the phase transformation of Al_2O_3 and the growth of Al_2O_3 grains break the extremely thin and ductile Au nano-layers. The damage of the Au multi-sealed nano-layers will certainly decrease the oxidation resistance of the A-G laminated coating. While, the doped Au particles and platelets will absorb and release the crack driving stress by their plastic deformation and crack bridging effect [28].

Therefore, the A-G laminated composite coatings can still provide much better mechanical property under cyclic oxidation test as no cracks or spallations are observed.

Figure 6 shows the composition of the oxide scales of the samples after cyclic oxidation. It is verified that most of the formed oxide scale on the uncoated TiAl-based alloy substrate fall off because the strong peaks are identified as alloy phase. The word "completely" seems to be too strong, because some minor oxides peaks are also identified.

Besides, only α-Al_2O_3 phase is identified, which indicates that most of the Al_2O_3 (amorphous, θ, γ) has transformed to crystalline α-Al_2O_3. Can you say "completely transformed"? An amorphous phase cannot be detected by XRD.

3.4 Mechanical Properties of Oxide Scales and Coatings after Oxidation Test

The novel Al_2O_3Au laminated composite coatings are designed to be used in increasingly demanding applications which require both good oxidation and spallation resistance at high temperatures. Experimental result of cyclic oxidation test exhibits that the surface protective A-G laminated coatings can still maintain good adhesion with substrate under the thermal stress and the growth stress of the oxide scales. It is indicated that the prepared A-G laminated coatings in this study can effectively resist internal stress. In addition, after oxidation test the adhesions of the formed oxide scales of all samples to TiAl-based alloy substrates were analyzed by scratching adhesion tester system (model MFT-4000) at room temperature. The scratch test exploits the normal force range from 1 N to 40 N. The loading speed is 20 N/min and the diamond indenter diameter is 0.4 mm. The frictional force and acoustic emission signals during scratching are recorded to determine the critical load of the oxide scale. Figure 7 (a) shows the scratching test results of the oxide scale of the sample coated with the three layers A-G laminated composite coating after cyclic oxidation test. It is seen that the first flex point of the friction force

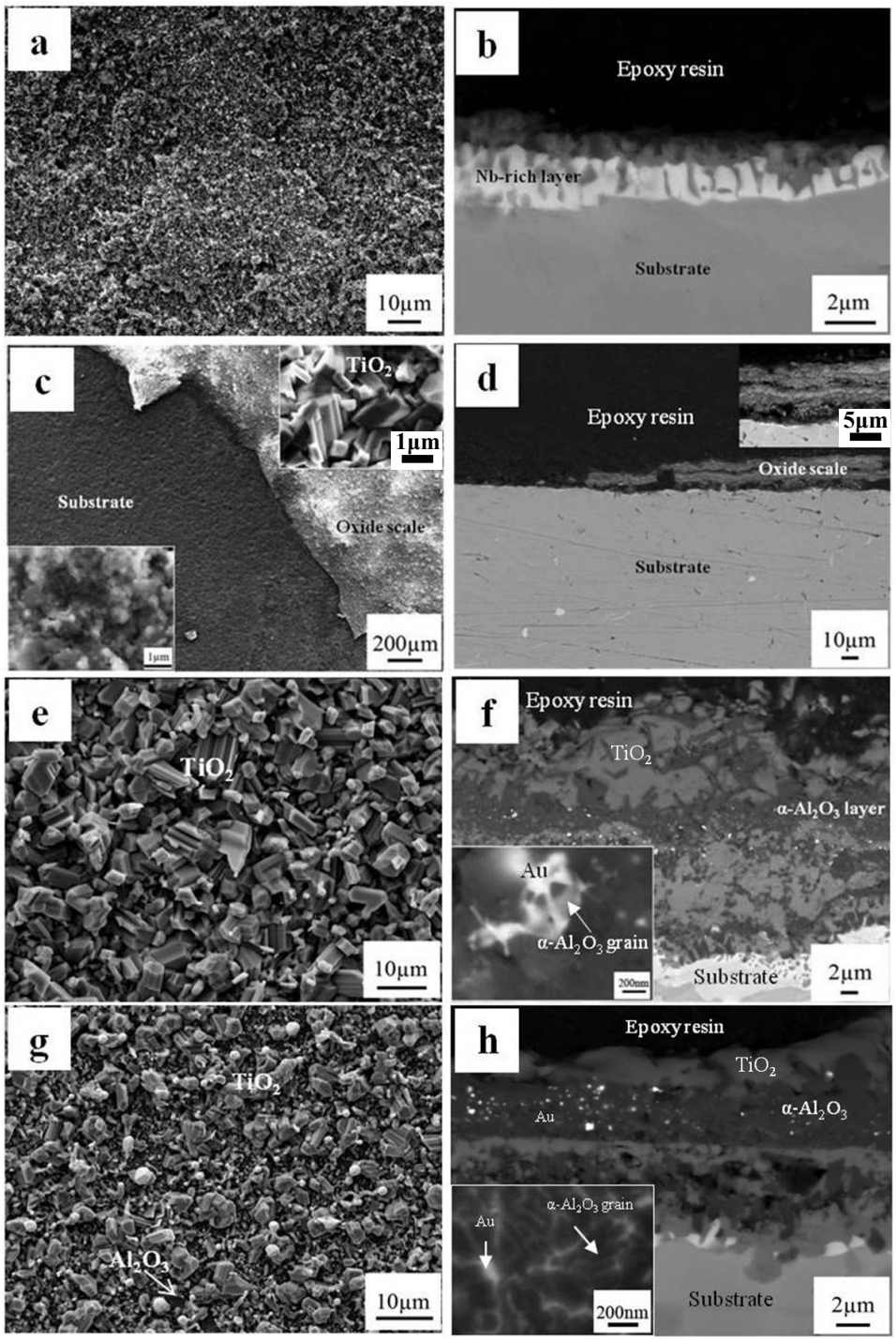

Figure 5. FE-SEM morphologies of samples with: Uncoated (a) surface, (b) cross-section; single Al_2O_3 coating (c) surface, (d) cross-section; three layers coating (e) surface, (f) cross-section and five layers coating (g) surface, (h) cross-section after cyclic oxidation at 900 °C for 200 h.

(Ff) curves and the acoustic emission signal (AE) curves coincide at the load of ~6 N. That is because the sound generated by the remarkable breakage of oxide scale leads to the abrupt change of the received acoustic emission signal. And at the same time, the indenter will reach to the TiAl-based alloy substrate which results in the critical condition of frictional force. So, the critical load of the formed composite oxide scale of the TiAl-based alloy coated with

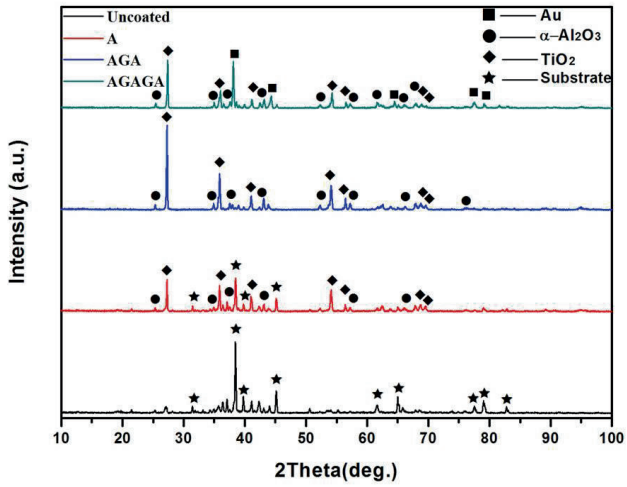

Figure 6. XRD spectra of samples uncoated and coated with a single Al_2O_3 coating, three layers and five layers A-G laminated composite coatings after cyclic oxidation test.

three layers A-G laminated composite coating could be determined as 6 N. Furthermore, to confirm the critical damage load of the formed oxide film more accurately, the surface SEM morphology (Figure 7 (b)) of the scratch mark is compared. In Figure 7 (b), the formed oxide scale breaks down at the point where the distance between the beginning of the scratch mark and the failure point of the oxide scale is one quarter of the length of the scratch mark. As it is known that the friction force and the acoustic emission signal were received simultaneously as the scratch test went on, the critical load of the oxide scale should be a quarter of the maximum load theoretically, which has been verified as shown in Figure 7 (a). Consequently, the critical load of the formed composite oxide scale of the TiAl-based alloy coated with three layers A-G laminated composite coating is 6 N.

Table 2 shows the critical loads of the formed oxide scales of all the samples after cyclic oxidation test at 900 °C for 200 h It is concluded that the adhesion of the oxide scale and TiAl-based alloy substrate is improved significantly by the A-G laminated composite coatings and the more layers the composite coating has, the better spallation resistance it provides.

4 Discussions

Experimental results indicated that the Al_2O_3-Au laminated composite coatings prepared by Magnetron Sputtering can significantly improve the spallation and oxidation resistance of TiAl-based alloy at high temperatures. The detailed mechanism models are discussed below.

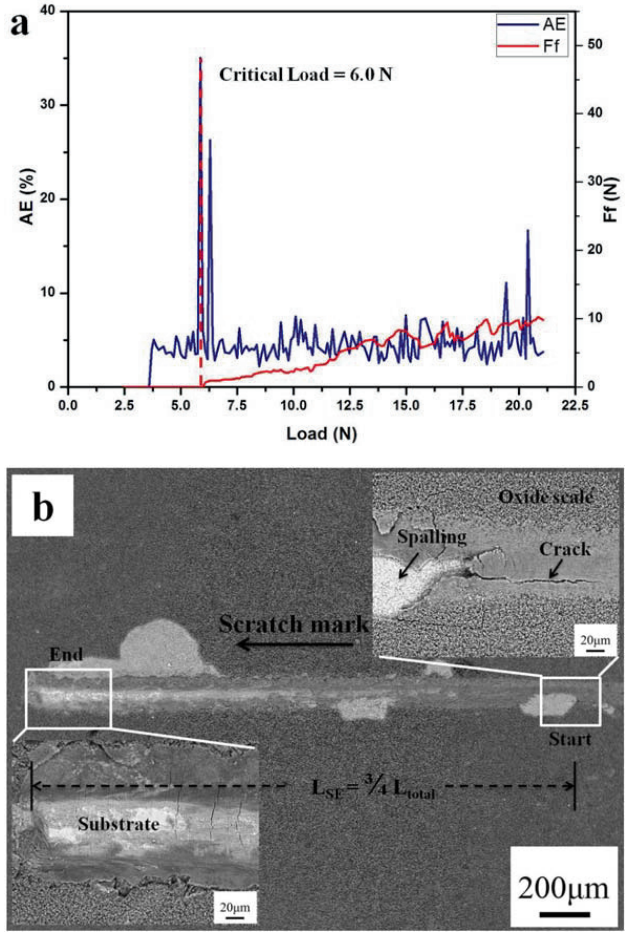

Figure 7. The friction force curves (Ff) and the acoustic emission signal curves (AE) (a) and the surface SEM images (b) of the oxide scale of the sample coated with the three layers A-G laminated composite coating after cyclic oxidation test at room temperature.

4.1 The Influence of the Number of Layers on Oxidation and Spallation Resistance of A-G Laminated Composite Coatings

High-temperature cyclic oxidation test has shown that the more layers the A-G laminated composite coating has the better oxidation resistance This can be explained by the "Sealing Mechanism" proposed in this study. In order to improve the oxidation resistance of the TiAl-based alloy, we propose a "Sealing mechanism" for designing the surface protective composite oxide scales or coatings. Such oxide scales or coatings should have a special structure, in which at least one phase with the lowest oxygen diffusion coefficient could seal the alloy substrate. In this work, the designed A-G laminated composite coatings consist of thermodynamically stable α-Al_2O_3 and Au phases which have very low oxygen diffusion coefficients. So that such laminated coatings have a laminated structure, in which both

Coatings	Critical load of oxide scale
Uncoated TiAl-based alloy	~0 N
Single Al_2O_3 coating	~2 N
Three layers A-G laminated composite coating	~6 N
Five layers A-G laminated composite coating	~9 N

Table 2. Critical loads of the formed oxide scales of samples after cyclic oxidation test at 900 °C for 200 h.

the α-Al_2O_3 and Au phases could seal the TiAl-based alloy substrate. And as the five layers A-G laminated coating has one more α-Al_2O_3 layer and one more Au layer than the three layers A-G laminated coating, it can provide the better oxidation resistance.

Besides, it is also revealed that the five layers A-G laminated composite coating exhibit not only excellent oxidation resistance but also better spallation resistance under thermal cycling (Figure 4 (a)). That is because the five layers A-G laminated composite coating has two more α-Al_2O_3/Au interfaces and the strength and fracture toughness of the formed oxide scales are improved due to the crack deflection or bifurcation at the α-Al_2O_3/Au interfaces. Also, the one more brittle Al_2O_3 layer can maintain the composite coating higher strength and the one more ductile Au layer probably can shield the more crack tips by the plastic deformation of ductile ligaments. Therefore, the fracture resistance of the five layers A-G laminated coating is increased. Furthermore, the level of thermal stress in this coating should be decreased comparing with the single phase Al_2O_3 coating and the three layers A-G laminated composite coating due to the lower Young's modulus and higher thermal- expansion coefficient (it is measured that the mass percent of Au in five layers A-G laminated composite coating is larger than the single phase Al_2O_3 coating and the three layers A-G laminated composite coating). It is concluded that the two conditions to improve the spallation resistance of sample coated with five layers A-G laminated composite coating are the increasing fracture resistance that permits the oxide scale to withstand bigger stresses, and decreasing the stress in oxide scales by increasing the thermal-expansion coefficient. Based on the above analysis, the five layers A-G laminated composite coating showed superior oxidation resistance and mechanical properties, we believed that the beneficial effects can be attributed to the brittle/ductile laminated structure with more layers.

4.2 The Ideal Mechanism Model for Oxidation and Spallation Resistance of A-G Laminated Composite Coatings

Firstly, α-Al_2O_3 and Au which have very low oxygen diffusion coefficients (ODC) are considered as ideal oxygen diffusion barrier materials. Therefore, the defect-free multi-sealed A-G laminated coatings prepared can prevent the oxidation of the TiAl-based alloy completely. Secondly, compared with a single Al_2O_3 coating, the CTE of A-G laminated coating is much closer to that of the alloy substrate [29], so that the thermal stress at the coating-substrate interface decreased and the thermal shock resistance of the samples can be improved during the cyclic oxidation test [30]. Thirdly, the brittle (Al_2O_3)/ductile (Au) laminated structure can prevent the crack propagation by means of energy release mechanisms [31]. The brittle Al_2O_3 micro-layers can provide sufficient strength for the laminated structure. The plastic deformation of ductile Au ligaments can absorb the impact stress caused by the mismatch in CTE and the growth stress of the α-Al_2O_3 grains during the cyclic oxidation, exhibits effective toughness. Therefore, the brittle/ductile structure ensures the A-G laminated coatings excellent flaw tolerance and crack resistance. Furthermore, as the thickness of each layer reaches to nanoscale with fine structure, it may give rise to the superplasticity of the laminated coating, which can also relax the thermal stress and improve the spallation resistance. Above all, in ideal condition, the A-G laminated composite coatings should completely protect the TiAl-based alloy from oxidation and spallation.

4.3 The Proposed Mechanism Model for Oxidation and Spallation Resistance of A-G Laminated Composite Coatings

The oxidation weight gain and spallation mass of samples with A-G laminated coatings are observed after the cyclic oxidation. Therefore, it is necessary to introduce a real mechanism model as shown in Figure 8 to expound and analyze the experimental results which made a deviation from theoretical value.

At the initial stage of cyclic oxidation test (Figure 8 (a)), the amorphous Al_2O_3 hasn't completely transformed to α-Al_2O_3. Therefore, the multi-sealed Al_2O_3 micro-layers could not prevent the oxidation of TiAl effectively. Then the Au nano-layers which have much smaller ODC will play the dominated role in preventing the diffusion of oxygen. The oxidation kinetics (Stage No. 1 in Figure 4) can verify that the inward diffusion of oxygen can be suppressed to an extremely low level by the Au nano-layers. Simultaneously,

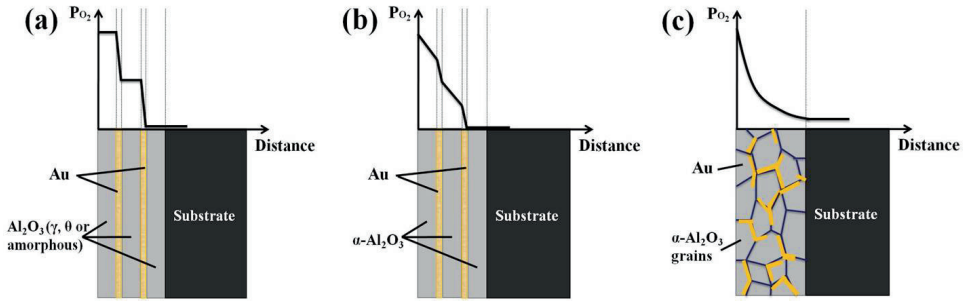

Figure 8. The proposed mechanism model of oxidation and spallation resistance of A-G laminated composite coatings: (a) the initial stage, (b) the mid-stage, (c) the 3rd stage.

no spallation mass is viewed in the initial stage because the defect-free brittle/ductile A-G laminated structure can exhibit high toughness and good adhesion. Moreover, it is known that the amorphous Al_2O_3 layers could function as a barrier layer against oxygen diffusion only within a limited range of heat treatment conditions. Therefore, in this work, the initial stage of the cyclic oxidation test can be seen as the heat treatment.

At the mid-stage (Figure 8 (b)), the oxidation resistance of the laminated coatings results from the combined action of the α-Al_2O_3 and Au layers because the amorphous Al_2O_3 has already transformed to α-Al_2O_3. So, the A-G laminated composite coatings could provide the best oxidation resistance in this stage. Besides, the inner stress can be absorbed by the brittle/ductile laminated structure and the cracks in oxide scales are shielded and avoided. Therefore, it can be seen that spallation mass and weight gain remain relatively stable in this stage (Stage No. 2 in Figure 4).

At the 3rd stage (Figure 8 (c)), it is viewed that the oxidation kinetics of samples coated with five layers A-G laminated composite coatings is almost constant (Stage No. 3 in Figure 4 (b)) and this can be explained as follows. The weight gain for the AGAGA sample is almost constant during the 3rd stage. Is it a linear law?

According to the experimental results, the growth kinetics of thermal growth oxide scale (TGO) on uncoated TiAl-based alloy follows the parabolic law It may be assumed that the oxygen barrier efficiency of the supplied A-G laminated composite coatings on the surface of TiAl-based alloy is equivalent to a TGO with the thickness, x_0, grew for time t_0,

$$x_0^2 = k t_0. \tag{1}$$

So, the thickness, x, of TGO on TiAl-based alloy covered with A-G laminated composite coatings is the function of time, t, and can be written as:

$$(x_0 + x)^2 = k(t_0 + t). \tag{2}$$

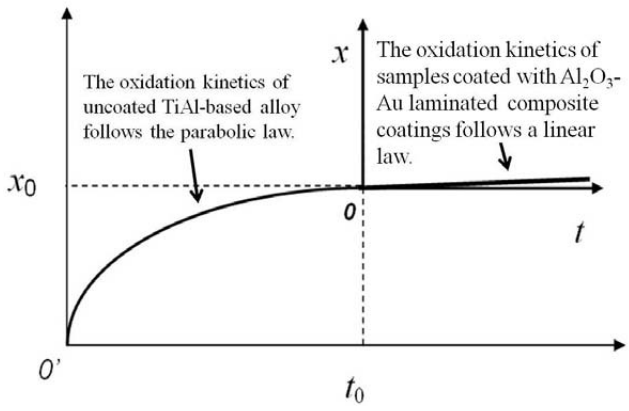

Figure 9. Theoretical growth kinetics of TGO of TiAl-based alloy coated with A-G laminated composite coatings.

Substitute equation (1) in equation (2):

$$2x_0 x + x^2 = kt. \tag{3}$$

As $x_0 \gg x$, equation (3) can be simplified as

$$2x_0 x \approx kt \quad \text{or } x \approx kt/2x_0. \tag{4}$$

Therefore, the growth kinetics of TGO on TiAl-based alloy covered with A-G laminated composite coatings follows a linear relation with time, as shown in Figure 9.

In addition, in this stage, the result reveals that a dense and continuous crystalline α-Al_2O_3 scale has formed and the Au nano-layers have been destroyed. And it is analyzed that the structural failure of the Au nanolayers is mainly owing to the increasing thermal stress and the growth stress generated in the coating.

However, the aggregation of Au at α-Al_2O_3 grain boundaries (detailed pictures in Figure 5 (f) and 5 (h)) could inhibit abnormal α-Al_2O_3 grain growth, hinder the grain boundary sliding and refine the grain size. So, according to Hall–Petch strengthening mechanism [32, 33] where the yield stress increment is inversely proportional to the square

root of the grain diameter, the strength and toughness of the α-Al_2O_3 layer and the formed oxide scale of the substrate can be improved. In conclusion, at the final stage, the oxide scales still have excellent mechanical property under huge cyclic thermal stress even though the laminated structure has been destroyed. Yet, the oxidation resistance of coating is worse than the previous stage because the Au layers destroy and fail to seal the substrate. In this case, TiO_2 is preferentially formed in the external scale (in Figure 5 (f) and 5 (h)) because TiO_2 is thermodynamically more stable than Al_2O_3 [34]. While the diffusion of oxygen along α-Al_2O_3 grain boundaries is accelerated by the Au particles and platelets segregated at the α-Al_2O_3 grain boundary areas. And the diffusion of oxygen in α-Al_2O_3 is very slow. Therefore, α-Al_2O_3 scales doping with Au during high temperature oxidation of this stage can also effectively seal the substrate TiAl-based alloys from further oxidation.

5 Conclusions

In summary, uncoated TiAl-based alloy exhibited poor cyclic spallation and oxidation resistance at 900 °C and the deposited Al_2O_3 protective coating had limited capability to improve the cyclic oxidation resistance of TiAl due to the spallation. The novel Al_2O_3-Au laminated composite coatings prepared in this work significantly improved the high-temperature cyclic oxidation resistance of TiAl due to the "sealing mechanism" of α-Al_2O_3 and Au layers. The brittle/ductile laminated structure which provides good coating-substrate compatibility can effectively enhance the strength and toughness in combination with improved damage resistance of the composite coatings. Consequently, the adhesion of the oxides scales can be improved remarkably. The cost of Au is extremely low (Au layer is only 100 nm thick), which guarantees this novel coating economic feasibility of industrial application. Moreover, it is expected that alloying additions such as Pt and Rh in Au and minor doped Y_2O_3 and ZrO_2 in Al_2O_3 could avoid the structural failure of Al_2O_3-Au laminated coating and improve the high-temperature oxidation resistance and mechanical properties of the Al_2O_3-Au laminated coating. A further investigation on this topic is currently under way.

Acknowledgments

The authors thank the financial support from the Chinese National Nature Science Foundation (Grant 51071030).

References

[1] C. T. Yang, C. H. Koo, Intermetallics 12 (2004) 235–251.
[2] Y. W. Kim, JOM. 46 (1994) 30–39.
[3] Y. W. Kim, Acta Metall. Mater. 40 (1992) 1121–1134.
[4] K. L. Luthra, Oxide. Met. 36 (1991) 475.
[5] Y. Shida, H. Anada, Oxid. Met. 45 (1996) 197–219.
[6] P. R. Subramanian, M. G. Mendiratta, D. M. Dimiduk, JOM. 48 (1996) 33–38.
[7] Y. H. Wang, J. P. Lin, Y. H. He, Y. L. Wang, G. L. Chen, Mater Sci Eng A. 471 (2007) 82–87.
[8] Y. Shida, H. Anada, Mater. Trans. JIM. 35 (1994) 623.
[9] R. L. McCarron, J. C. Schaeffer, G. H. Meier, D. Berztiss, R. A. Perkins, J. Cullinan, in: F. H. Froes, I. Caplan (Eds.), Titanium'92, TMS, Warrendale, PA, 1993, p. 1971.
[10] M. P. Brady, W. J. Brindley, J. L. Smialek, I. E. Locci, J. Organomet. Chem. 48 (1996) 46.
[11] Z. Tang, F. Wang, W. Wu, Surf. Coat. Technol. 110 (1998) 57–61.
[12] P. Y. Théry, M. Poulain, M. Dupeux, M. Braccini, J. Mater. Sci. 44 (2009) 1726–1733.
[13] M. Fröhlich, R. Braun, C. Leyens, Surf. Coat. Technol. 201 (2006) 3911–3917.
[14] S. Taniguchi, T. Shibada, T. Yamada, X. Liu, S. Zou, ISIJ Int. 33 (1993) 869.
[15] S. Taniguchi, T. Shibada, N. Katoh, J. Jpn. Inst. Met. 57 (1993) 666.
[16] S. Taniguchi, T. Shibada, K. Takeuchi, Mater. Trans. JIM. 32 (1991) 299.
[17] Z. Tang, L. Niewolak, V. Shemet, Mater. Sci. Eng. A 328 (2002) 297–301.
[18] H. E. Evans, Mater. Sci. Eng. Vol. A 120 (1989), p.139.
[19] M. Schütze, M. Malessa, D. Renusch, P. F. Tortorelli, I. G. Wright, and R. B. Dooley, Mater. Sci. Forum Vol. 522–523(2006), p.393.
[20] H. Mao, S. Mahadevan, Compos. Struct. 58 (2002) 405–410.
[21] A. R. Boccaccini, V. Winkler, Composites: Part A 33 (2002) 125–131.
[22] M. Yao, Y. He, D. Wang, W. Gao, Rare Earth 23 (2005) 559.
[23] Y. He, J. Gao, C. Ren, D. Wang, J. Zhang, Chinese Patent ZL200910084729.0 (2009).
[24] J. Gao, Y. He, D. Wang, Mater. Chem. Phys. 123 (2010) 731–736.
[25] T. Charatier, T. Rouxel, J. Euro. Ceram. 17 (1997) 299–308.
[26] Toshihide Nabatame, Tetsuji Yasuda, Jpn. J. Appl. Phys. 42 (2003) 7205–7208.
[27] R. I. Jaffee, D. J. Maykuth, Refractory materials, DMIC Memorandum.
[28] M. T. Tilbrook, I. E. Reimanis, K. Rozenburg, M. Hoffman, Acta Mater. 53 (2005) 3935–3949.
[29] P. S. Turner, Journal of Research of NBS. 37 (1946) 39.
[30] N. Birks, G. H. Meier, F. S. Pettit, Introduction to the high-temperature oxidation of metals, 2nd ed., New York, Cambridge University Press, 2006: 139.
[31] R. Bermejo, J. Pascual, T. Lube, R. Danzer, J. Eur. Ceram. Soc. 28 (2008) 1575.
[32] E. O. Hall, Proc. Phys. Soc. B. 64 (1952) 747.
[33] N. J. Petch, J. Iron Steel Inst. 174 (1953) 25.
[34] A. Rahmel, P. J. Spencer, Oxide. Met. 35 (1/2) (1991) 53.